

M.P. BOGANA¹
L. COLOMBO²,✉

Atomic scale simulations of vapor cooled carbon clusters

¹ NEMAS (Center of Excellence for NanoEngineered Materials and Surfaces),
Dipartimento Ingegneria Nucleare, Politecnico di Milano, via Ponzio 34/3, 20133 Milano, Italy
² Dipartimento di Fisica and DEMOCRITOS National Simulation Center and SLACS Laboratory
(CNR-INFN), Università di Cagliari, Cittadella Universitaria, 09042 Monserrato (Ca), Italy

Received: 10 August 2006/Accepted: 12 October 2006
Published online: 18 November 2006 • © Springer-Verlag 2006

ABSTRACT By means of atomistic simulations we observed the formation of many topologically non-equivalent carbon clusters formed by the condensation of liquid droplets, including: (i) standard fullerenes and onion-like structures, (ii) clusters showing extremely complex surfaces with both positive and negative curvatures and (iii) complex endohedral structures. In this work we offer a thorough structural characterization of the above systems, as well as an attempt to correlate the resulting structure to the actual protocol of growth. The IR and Raman responses of some exotic linear carbon structures have been further investigated, finding good agreement with experimental evidence of carbinoid structures in cluster-assembled films. Towards the aim of fully understanding the process of cluster-to-cluster coalescence dynamics, we further simulated an aerosol of amorphous carbon clusters at controlled temperatures. Various annealing temperatures and times have been observed, identifying different pathways for cluster ripening, ranging from simple coalescence to extensive reconstruction.

PACS 36.40; 61.43.Bn, 61.48.+c; 81.05.Tp

1 Introduction

Carbon-based structures can be roughly divided into two large families: the first containing high-symmetry clusters (HSC) (e.g. fullerenes or tube-like molecules) and the second containing the huge variety of amorphous clusters (AC). While the nucleation dynamics and the equilibrium morphology of HSC have been extensively investigated in recent years [1, 2], little is known about amorphous carbon clusters. Interest in amorphous cluster structures has recently increased, due to experimental reports about their extremely complex and still puzzling physical behavior. Recent experiments suggest, for example, the lack of specific ‘magic numbers’ in the mass distribution of cluster beams produced both by pulsed laser vaporization sources (PLVS) [3] and pulsed microplasma cluster sources (PMCS) [4–6]. As a matter of fact, almost comparable concentrations of both even- and odd-

membered clusters are observed [3]. PMCS, in particular, provides clusters containing as many as 30–1000 atoms [5, 6]. Furthermore, materials grown by PMCS cluster assembling display intriguing structural features, like stable linear carbon chains [7–9]. It is guessed that both chain-like and foam-like structures are produced during the carbon vapor cooling process, depending on annealing conditions [4, 5]. The resulting clusters further grow giving rise to larger structures, which eventually are deposited on a substrate or filter.

This scenario defines the framework for the present computer-based study. By means of atomistic simulations, we investigated the condensation of liquid carbon droplets in different physical conditions. We observed the formation of many topologically non-equivalent carbon clusters, including: (i) standard fullerenes and onion-like structures, (ii) clusters showing extremely complex surfaces with both positive and negative curvatures, (iii) endohedral linear chain structures and (iv) many open topologies with truncated graphite-like structures. In this work we offer a thorough structural characterization of the above systems, as well as an attempt to correlate the resulting structure to the actual protocol of growth. Some exotic endohedral objects have been further investigated, finding excellent agreement between linear chain objects observed in simulated clusters and the experimental evidence of carbinoid structures in cluster-assembled films [7]. Towards the aim of fully understanding the process of cluster-to-cluster coalescence dynamics, we further simulated an aerosol of amorphous carbon clusters at controlled temperatures. By modifying annealing temperature and time we have observed different pathways for cluster ripening, ranging from simple coalescence to extensive reconstruction.

2 Computational framework

Cluster formation has been investigated by means of tight-binding molecular dynamics (TBMD) [10]. The basic idea of the TBMD scheme is to derive the interatomic forces governing the time evolution directly from the electronic structure of the simulated system. In order to reduce as much as possible the computational workload, the electronic structure is calculated in the framework of the semi-empirical

✉ Fax: +39 070 510171, E-mail: luciano.colombo@dsf.unica.it

tight-binding (TB) model. Assuming a frozen core picture for the electrons, we can write the total potential energy of the system of ion cores and valence electrons as

$$E_{\text{tot}} = U_{\text{ee}} + U_{\text{ei}} + U_{\text{ii}}, \quad (1)$$

where the electron–electron, electron–ion and ion–ion interactions are given by U_{ee} , U_{ei} and U_{ii} , respectively. Atomic trajectories are then generated by the TB Hamiltonian

$$H = \sum_{\alpha} \frac{p_{\alpha}^2}{2m_{\alpha}} + 2 \sum_n^{\text{(occup)}} \varepsilon_n + U_{\text{rep}}, \quad (2)$$

where the label α runs over the atoms in the simulation cell and the second sum is extended to those electron energies ε_n belonging to the lower half spectrum of the TB matrix. The effective repulsive potential $U_{\text{rep}} = U_{\text{ii}} - U_{\text{ee}}$ can be expressed as a sum of suitable two-body potentials $U_{\text{rep}} = \sum_{\alpha, \beta > \alpha} \Phi(R_{\alpha\beta})$, where $\Phi(R_{\alpha\beta})$ is guessed on the basis of physical intuition and numerical convenience for molecular dynamics applications. The free parameters appearing in $\Phi(R_{\alpha\beta})$ are usually determined together with those obtained in the scaling functions for the TB hopping integrals. The interatomic forces are derived by means of the Hellman–Feynman theorem, so that their many-body nature is naturally taken into account. In this work we used the TB model developed by Xu, Wang, Chan and Ho [11].

In order to study different carbon cluster topologies ranging from 60 to 300 atoms, we have

1. Prepared an initial spherical distribution (radius R) of n carbon atoms (density $\rho(n; R) = n/(4/3\pi R^3)^{-1}$). The initial atomic coordination has been imposed to be ≤ 3 and the interatomic distance is assumed $\geq 1.8 \text{ \AA}$. Different initial densities ρ of $1.8\text{--}2.5 \text{ g/cm}^3$ have been investigated.
2. On these initial configurations we have performed an energy minimization run in order to reach a local energy minimum.
3. The resulting structure is then heated to a very high temperature (e.g. $\sim 5000\text{--}6000 \text{ K}$) in order to produce its fragmentation in clusters of different dimensions: from small carbon molecules (e.g. dimers, trimers, etc.) to medium-size clusters C_n (e.g. $n \gg 30$ atoms). They will act as nucleation seeds.
4. At this point the carbon vapor is cooled to $2500\text{--}4000 \text{ K}$ in $100\text{--}160 \text{ ps}$ in order to observe cluster condensation (the simulation time step was 0.5 fs).

Our attention has then been focused on intercluster coalescence. In order to study systems involving more than a thousand atoms, we have switched from TB to model potential molecular dynamics (MPMD) as based on the Tersoff cohesion model [12, 13]. In the Tersoff MPMD picture, the system potential energy can be written as $E = 1/2 \sum_{i \neq j} V_{ij}$, where

$$V_{ij} = f_C(r_{ij})[a_{ij} f_R(r_{ij}) + b_{ij} f_A(r_{ij})], \quad (3)$$

and where f_R represents the repulsive pair potential, f_A the attractive pair potential and f_C a cutoff function, while b_{ij} is a function measuring the bond order and a_{ij} is a function limiting the interaction shell only to first neighbors.

A vapor of clusters, obtained by the previous TBMD model (1350 atoms in a simulation cell with 10^3 nm^3 volume) and further optimized in the Tersoff MPMD approximation, has then been annealed at temperatures ranging from 1000 K to 5000 K for a total simulation time of $0.3 \mu\text{s}$, observing intercluster coalescence dynamics.

3 Large cluster formation and characterization

During the condensation step we observed that an extensive microstructure evolution of carbon clusters occurs through both the modification of their topology and the absorption/desorption of small fragments from/to the surrounding vapor. As a result of these processes the system explores many local energy minima, whose stability is strongly correlated to specific thermodynamic parameters, like temperature, pressure, carbon vapor density and so on. From our simulations we observed that any significant cluster reconstruction dynamics is quenched at temperatures below 1500 K . For this reason we will here suppose that the system undergoes a rapid cooling below 2000 K . The stabilized intermediate cluster structures will contribute to the final cluster population, appearing in mass spectra [4]. Obviously other thermodynamic parameters like buffer-gas pressure, supersonic expansions, turbulence, etc. will contribute to the final cluster topology. Nevertheless, in the present study we will discard all these parameters, assuming as a first approximation that the main driving force to cluster nucleation is the annealing temperature.

3.1 Open, nautilus-like and closed clusters

By focusing on temperatures of $2500\text{--}3500 \text{ K}$, three main families of metastable cluster structures can be identified: open clusters, nautilus-like clusters and closed clusters.

Open clusters (O) (see Fig. 1a–c) are basically small graphite sheets presenting a local curvature induced by specific graphite-like network defects (e.g. five, seven or even more complex defects). According to the curvature these clusters can be divided into two sub-families: low-curvature (Lc) open clusters (e.g. almost flat graphite sheets, see Fig. 1a) or high-curvature (Hc) open clusters (e.g. open fullerenes, see Fig. 1b), or complex involuted structures, see Fig. 1c).

Nautilus-like clusters (N) (see Fig. 1g–i) are formed by graphite-like shells curled on themselves one or more times, forming a structure similar to a nautilus shell topology. These objects had been guessed in 1986 by Kroto and Smalley as intermediate states along the path to large fullerenes [14]. Nevertheless, to our knowledge this is the first time they have been observed nucleating from a pure carbon vapor without any initial guess.

Closed clusters (C) (see Fig. 1d–f) are characterized in general by one or more graphite-like closed shells. Although these shells have no high-symmetry topology like C_{60} buckminsterfullerene, they are nevertheless extremely stable even under high-temperature annealing. As Maruyama and Yamaguchi reported [2], clusters must undergo a long annealing ($> 200 \text{ ns}$) at temperatures above 2500 K in order to evolve towards high-symmetry topologies.

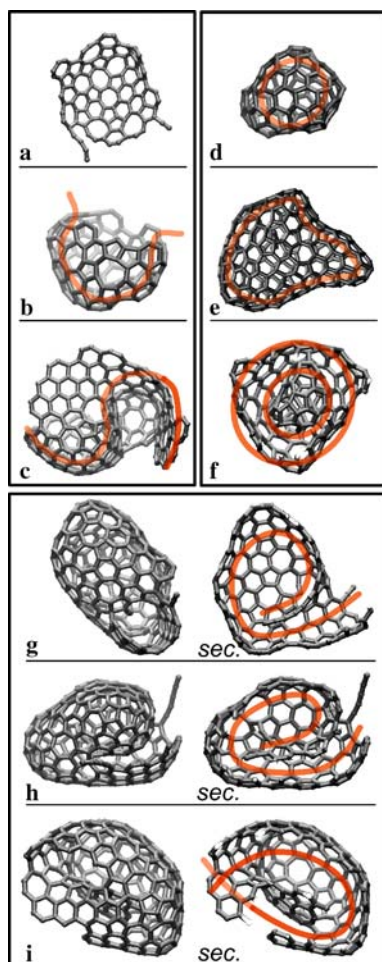


FIGURE 1 Examples of clusters of the open (a–c), nautilus-like (d–f) and closed (g–i) families

By reducing the system temperature below 2000 K along the nucleation path, both O cluster and N cluster topologies can be frozen. Nevertheless, we observe that O and C clusters may further grow by adding small carbon molecules from the surrounding vapor and by modifying their internal curvatures. An example is reported in Fig. 2. In this case we observe the transition of an O cluster towards a C cluster passing through an N cluster structure during a 3000 K annealing. On the other hand, not all N and O clusters investigated by our simulations evolve towards C clusters. Rather, we see that some of them keep on growing by absorbing small carbon molecules from the carbon vapor. As we see, for example in Fig. 3, small chains can be absorbed and embedded in the graphite-like network in less than 0.5 ps. Acting in this way, graphite sheets can grow up to a micrometric size or N clusters can increase their number of swirls.

Interesting enough, no distinction exists between even- and odd-membered clusters of the O and N families. Conversely, our simulations report only even-membered C clusters.

3.2 Linear cluster defects and endohedral structures

All previous families of clusters can be considered a sort of complex graphite-like network presenting a given

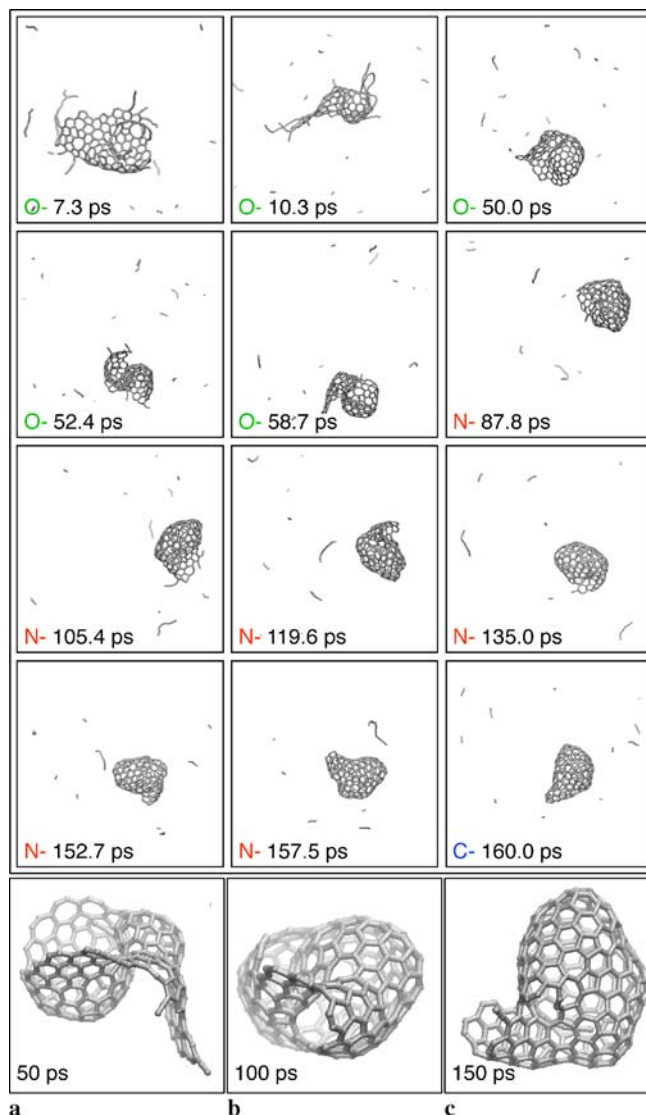


FIGURE 2 Evolution of a 300-atom system during a 3000 K annealing. Simulation time and main cluster family for each frame are reported in the *lower left corner* of the frame: (O) → open, (N) → nautilus-like and (C) → closed. Three main intermediate states along the final (C) structure at 160 ps are reported in (a), (b) and (c)

curvature and folding. Nevertheless, we know from experimental evidence that more complex cluster topologies, with high concentrations of linear carbon chain structures, can be stabilized in a PMCS source [4]. Similar extensive linear chain structures have been observed also in our simulations. They are characterized by linear chains possibly entangled or linking nearby graphite-like fragments. Despite the complexity and variety of these networks, we can classify such structures as follows:

1. linear chains external to cluster surface (i.e. ‘hairy fullerenes’ like in Fig. 4a),
2. linear structures on cluster surface (Fig. 4b),
3. complex endohedral linear chains confined to the cluster graphite-like shell (Fig. 4c).

‘Hairy fullerenes’ present long linear chains anchored to external shell defects like adatoms. Simulations show also that

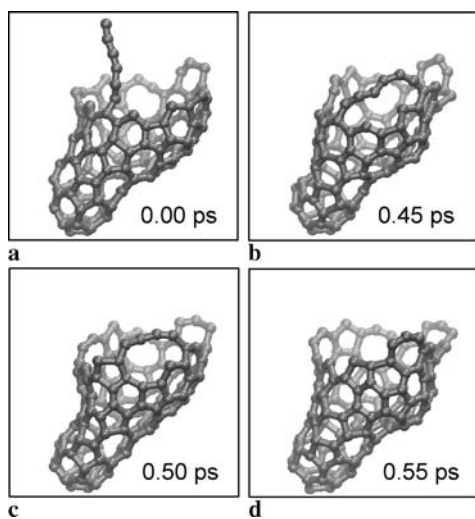


FIGURE 3 Rapid degeneration (~ 0.55 ps) of a linear carbon chain C_6 adsorbed on the border of a local graphite-like cluster O at 2500 K

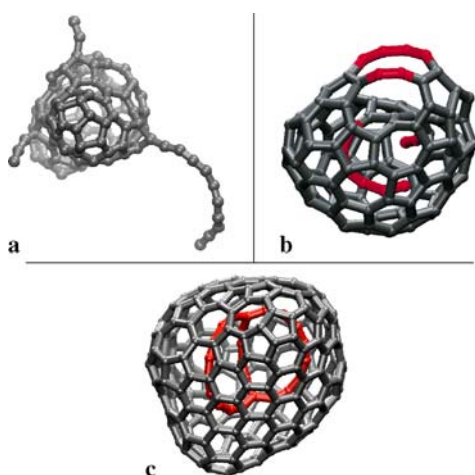


FIGURE 4 Three examples of linear carbon chains in a carbon cluster: (a) 'hairy fullerene', (b) shell defect and (c) endohedral structure

these linear chains are not strongly bonded on the cluster surface, but can easily stick or detach.

Quite different is the behavior of linear chains lying on the outer surface of a shell (Fig. 4b). Simulations reveal that chains stabilized in this way are extremely stable even at temperatures above 2000 K. Only at temperatures above 2500 K did we observe that such objects rapidly evolve by forming a more stable graphite-like network.

Much more complex is the situation for endohedral structures. These structures are composed of carbon networks of graphitic fragments and linear chains. These networks are confined inside an otherwise stable shell. Thanks to the volume confinement imposed by the external shell, endohedral structures can assume very peculiar topologies that are extremely stable even under long annealing at temperatures above 2500 K.

Depending on the number of carbon atoms in the linear chains or in the graphitic fragments, we have observed different behaviors. As we can see from Fig. 5, a graphitic fragment under high-temperature annealing naturally may evolve towards a more stable linear network of carbon atoms. During

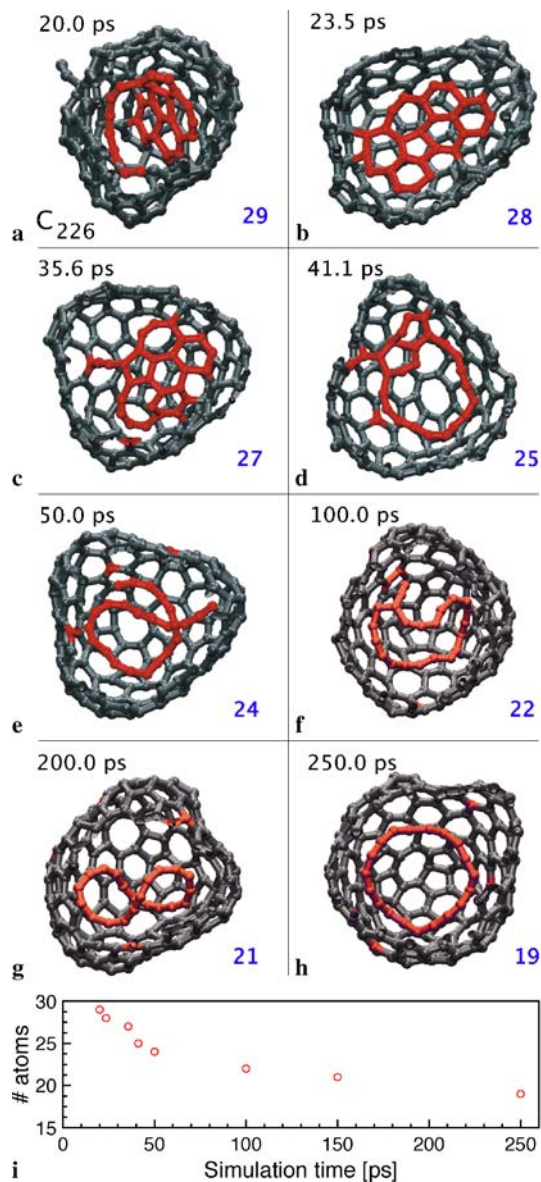


FIGURE 5 Evolution of a C_{226} C cluster with an endohedral structure during a 3000 K annealing. Initial endohedral structure atoms ($\tau_{\text{anneal}} = 0$ ps) are highlighted in red. Endohedral structure mass during annealing is reported in the lower right corner of each frame. Annealing time is reported in the upper left corner of each frame. In (i) a plot of the number of atoms belonging to the endohedral structure versus simulation time (in ps) is reported

this process we observe the drift of some atoms from the endohedral structure towards the external shell (red atoms traced in Fig. 5). Most likely the endohedral structure in its initial configuration is not free to evolve because of spatial confinement. However, if some carbon atoms drift to the shell surface more room is created for its microstructure evolution, which eventually drives the formation of linear objects as shown in Fig. 5.

Obviously all these phenomena are strongly related to annealing temperature. Below 2500 K, almost all intermediate states previously observed (e.g. Fig. 5a–h) can be stabilized. It is clear from this point of view that a linear carbon chain (pure sp carbon structure), confined in a carbon nanotube (highly sp^2 shell), is the most stable example of an endohedral

structure. Systems of this kind have been recently experimentally observed in High-Resolution Transmission Electron Microscopy (HR-TEM) images [15].

4 Raman spectra of chain-like structures

Recent experimental investigations report such carbon chain networks using Raman spectroscopy techniques [16, 17].

In order to investigate the infrared (IR) and Raman responses of the linear chains, we have extracted such fragments from the TBMD-generated clusters. We decorated them with hydrogen atoms so as to saturate dangling bonds. Finally, the geometry of H-terminated structures has been fully optimized by means of Gaussian 03 [18] in a hybrid B3LYP density functional model along with a standard Pople's 6-311G** basis set (HDFE). Structural optimization has been obtained by first looking for equilibrium hydrogen positions at clamped carbon positions. Then carbon positions have been relaxed keeping hydrogen positions fixed, in order to mimic the surrounding cluster environment. The same Gaussian 03 package has then been used to evaluate the Raman and IR spectra. Original TBMD-generated clusters and the fully optimized

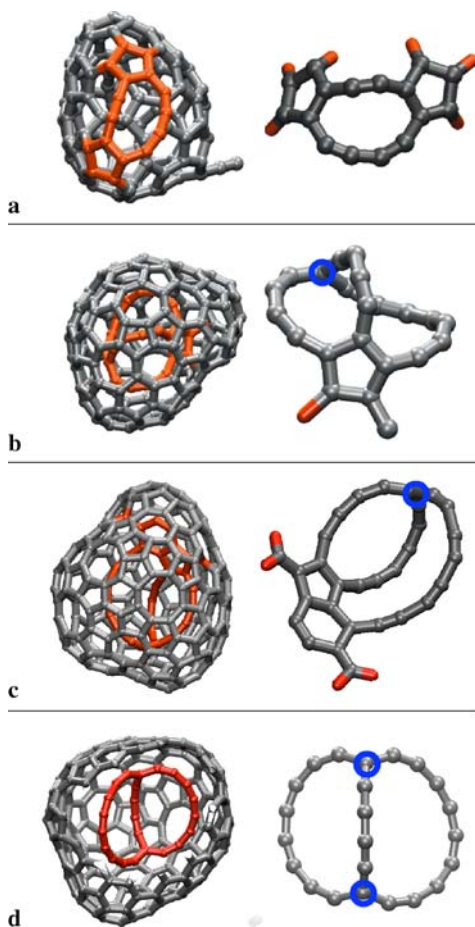


FIGURE 6 Complete cluster structure and the extracted fragments with hydrogen (red): linear cluster shell defects (a) and endohedral structure linear networks (b–d). For endohedral structures, in order to mimic the external graphite-like shell confinement, we fixed the positions of carbon atoms highlighted in blue

H-truncated fragments are shown in Fig. 6. It is important to notice that only small deviations have been observed between the TBMD and Gaussian 03 optimized structures.

The resulting Raman and IR spectra are reported in Figs. 7 and 8, respectively. Raman mode localization reveals that three main regions can be distinguished: modes at frequencies ω above 1700 cm^{-1} , of $1000\text{--}1750\text{ cm}^{-1}$ and under 1000 cm^{-1} . Modes above 1750 cm^{-1} are associated with the stretching modes of the chains. Those of $1000\text{--}1750\text{ cm}^{-1}$ are mainly associated with the graphite-like network modes. Modes below 1000 cm^{-1} are mainly due to bending modes. The same three regions can be identified in IR spectra in Fig. 8.

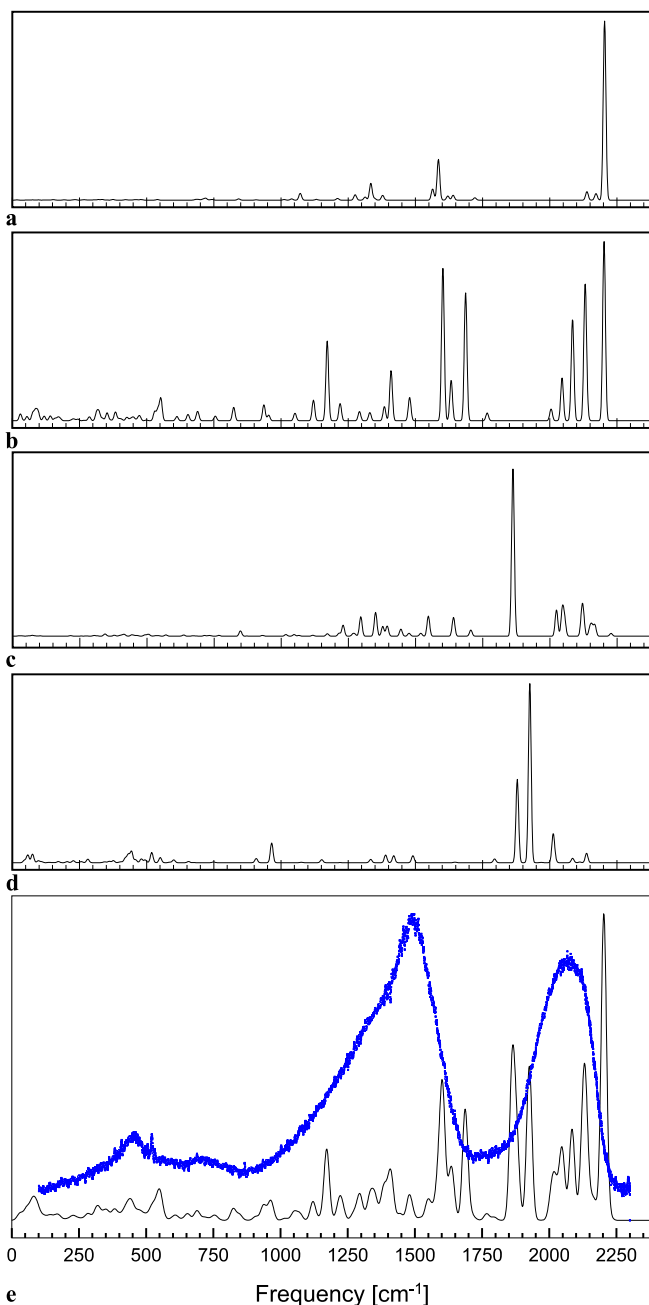


FIGURE 7 Raman spectra of structures in Fig. 6. In (e) there is reported the total Raman response of (a–d) and experimental results (blue) [4]

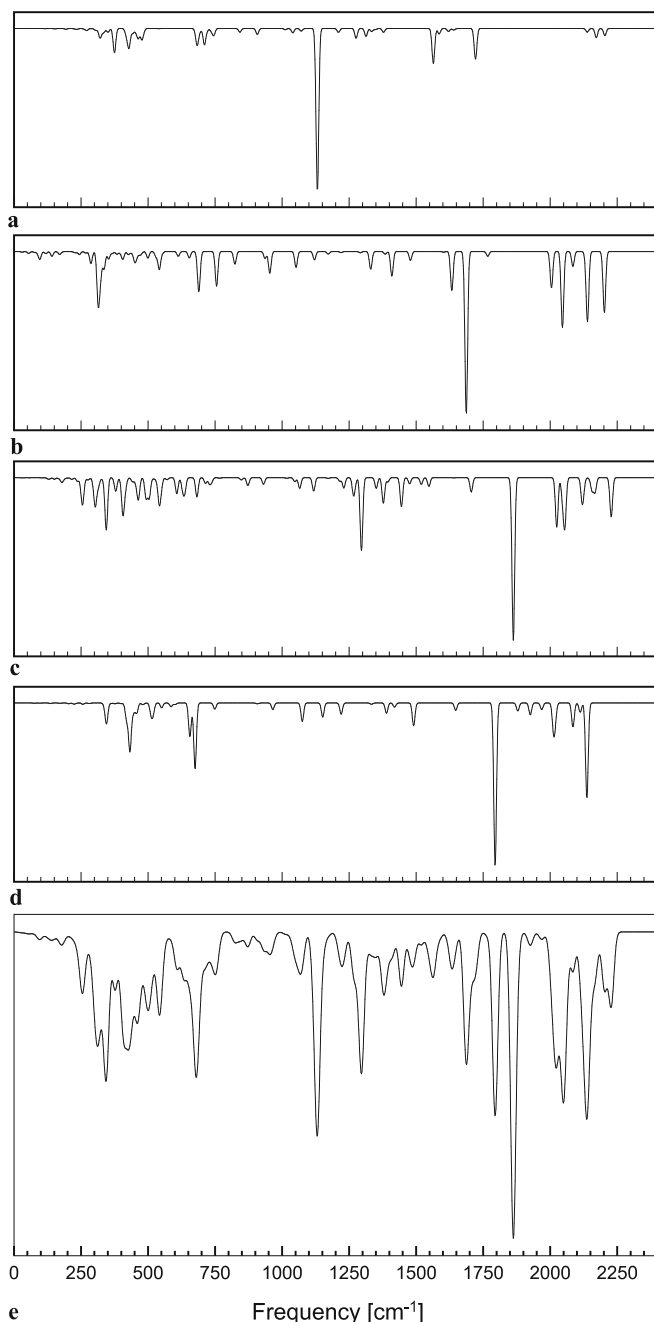


FIGURE 8 IR spectra of linear cluster shell defects (**a**) and endohedral structure linear networks (**b–d**). Complete cluster structures and corresponding endohedral substructures are reported in Fig. 6

In order to offer a direct comparison with experimental results [3,4], we have reported in Fig. 7e the total Raman spectra of all objects here investigated. As we can see there is good agreement between experimental and theoretical data, although more quantitative information could only be obtained by investigating a much richer cluster family.

5 Coalescence and giant clusters

All clusters so far investigated contain less than 300 atoms. From experimental evidence [5,6] we know

that these clusters can coalesce, evolving towards more complex structures containing up to 1000 atoms and in a few cases even more. In order to investigate this coalescence process we have created a vapor of 1350 carbon atoms arranged in eight clusters obtained by previous TBMD investigations. The evolution of this system has been studied by means of a Tersoff MD model. Annealing at temperatures in the range 1000–5000 K has been investigated.

Simulation results are reported in Fig. 9. Depending on the temperature, clusters show different coalescence features. At 1000 K clusters agglomerate; however, no significant system reconstruction is observed: each single cluster is still recognizable in the final agglomerate. By increasing the temperature this behavior changes and above 3500 K we observe a complete reconstruction. In particular, at 4000 K we observe the formation of a topology close to an amorphous schwarzite structure. Indeed, similar structures are observed during nanofoam formation experiments, under physical conditions similar to those considered in this study [19]. Finally, at temperatures above 5000 K, the cluster undergoes a dramatic reconstruction process. Initial cluster morphologies have completely disappeared and we observe the for-

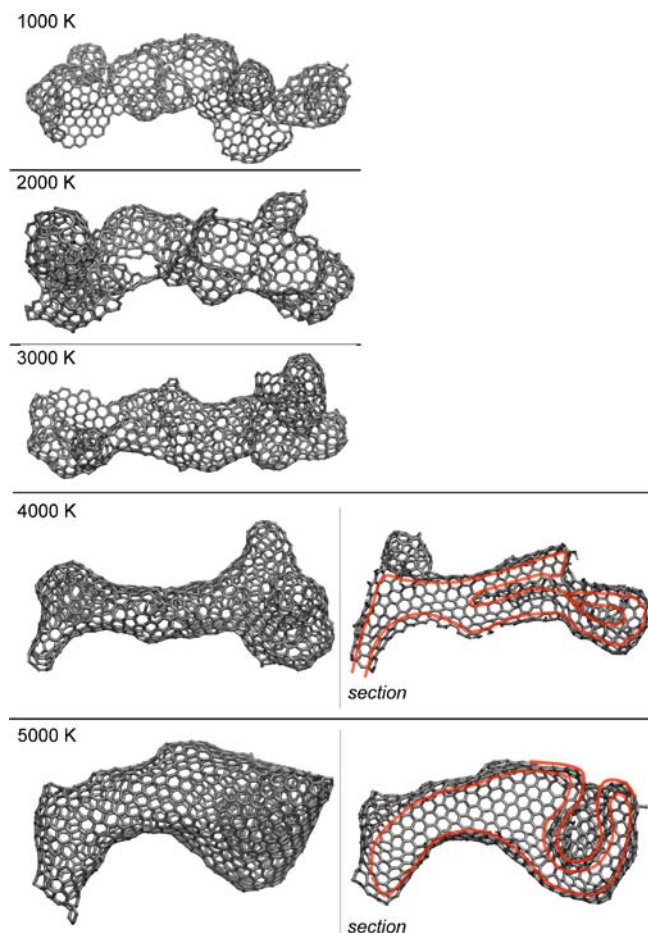


FIGURE 9 Giant C_{1350} fullerene structure at different annealing temperatures. Annealing temperatures are reported in the upper left corner of each cluster structure. For structures at 4000 K and 5000 K cluster sections are reported

mation of an onion-like topology, in line with many other experiments [20] and simulations [21].

6 Conclusions

We have investigated the carbon vapor cooling process and cluster nucleation dynamics by means of atomistic TBMD simulations. During this condensation process we have observed the formation and stabilization of complex amorphous carbon clusters that we have classified into three main families according to their shell topologies: (i) open clusters (O), (ii) nautilus clusters (N) and (iii) closed clusters (C). O clusters are basically small graphite sheets presenting a local curvature induced by specific graphite-like network defects. N clusters are characterized by complex graphite-like shells curled on themselves one or more times, forming a structure similar to a nautilus shell topology. Finally, C clusters show a fullerene-like topology, with one or more graphite-like shells closed on themselves (carbon onions).

We have observed that high temperature annealing conditions drive the evolution of both O and N clusters towards the C-cluster family, as predicted by fullerene nucleation dynamics studies [2]. In addition, we have reported the possibility of stabilizing these O- and N-cluster structures under low temperature annealing conditions (e.g. below 2000 K). At such a low-temperature regime we have also investigated the cluster growth dynamics by adding small carbon molecules and observing the stabilization of complex atomic linear chain networks.

In the case of rapid nucleation of massive C clusters (e.g. C_n with $n \gg 150$ atoms) we have observed the formation and stabilization of particular endohedral structures. They naturally evolve towards complex atomic linear chain networks during high-temperature annealing. Further investigation of the IR and Raman responses of these linear networks proved a good agreement with experimental evidence of carbinoid structures in cluster-assembled films [4, 16, 17].

Finally, in order to fully understand the process of cluster-to-cluster coalescence dynamics, we simulated an aerosol of amorphous carbon clusters at controlled temperatures. Modifying annealing temperature and time, we have observed different pathways for cluster ripening, ranging from simple coalescence to extensive reconstruction. These phenomena might be particularly important for example in the carbon onion [21] evolution dynamics and in the carbon nanofoam nucleation processes [19].

REFERENCES

- 1 R.E. Smalley, *Acc. Chem. Res.* **25**, 98 (1992)
- 2 S. Maruyama, Y. Yamaguchi, *Chem. Phys. Lett.* **286**, 343 (1998)
- 3 T. Wakabayashi, W. Krätschmer, *Polyynes: Synthesis, Properties, and Applications* (Taylor & Francis, Boca Raton, FL, 2006)
- 4 M. Bogana, L. Ravagnan, C.S. Casari, A. Zivelonghi, A. Baserga, A. Li Bassi, C.E. Bottani, S. Vinati, E. Salis, P. Piseri, E. Barborini, L. Colombo, P. Milani, *New J. Phys.* **7**, 81 (2005)
- 5 L. Ravagnan, Ph.D. dissertation, Department of Physics, University of Milano(I) (2005)
- 6 E. Salis, Ph.D. dissertation, Materials Engineering Department, Politecnico di Milano (2006)
- 7 E. Barborini, P. Piseri, P. Milani, *J. Phys. D: Appl. Phys.* **32**, 105 (1999)
- 8 T. Wakabayashi, A.L. Ong, D. Strelnikov, W. Krätschmer, private communication
- 9 T. Wakabayashi, M. Kato, Y. Yamaguchi, H. Kataura, S. Suzuki, Y. Achiba, Y. Tobe, T. Momose, K. Yoshimura, W. Krätschmer, *J. Phys. Chem. B*, unpublished
- 10 L. Colombo, *Riv. Nuovo Cimento* **28**, 1 (2005)
- 11 C.H. Xu, C.Z. Wang, C.T. Chan, K.M. Ho, *J. Phys.: Condens. Matter* **4**, 6047 (1992)
- 12 J. Tersoff, *Phys. Rev. Lett.* **56**, 632 (1986)
- 13 J. Tersoff, *Phys. Rev. Lett.* **61**, 2879 (1988)
- 14 Q.L. Zhang, S.C. O'Brien, J.R. Heath, Y. Liu, R.F. Curl, H.W. Kroto, R.E. Smalley, *J. Phys. Chem.* **90**, 525 (1986)
- 15 X. Zhao, Y. Ando, Y. Liu, M. Jinno, T. Suzuki, *Phys. Rev. Lett.* **90**, 187401 (2003)
- 16 L. Ravagnan, F. Siviero, C. Lenardi, P. Piseri, E. Barborini, P. Milani, C.S. Casari, A. Li Bassi, C.E. Bottani, *Phys. Rev. Lett.* **89**, 285506-1 (2002)
- 17 C.S. Casari, A. Li Bassi, L. Ravagnan, F. Siviero, C. Lenardi, P. Piseri, G. Bongiorno, C.E. Bottani, P. Milani, *Phys. Rev. B* **69**, 075422 (2004)
- 18 M.J. Frisch, G.W. Trucks, H.B. Schlegel, G.E. Scuseria, M.A. Robb, J.R. Cheeseman, J.A. Montgomery Jr., T. Vreven, K.N. Kudin, J.C. Burant, J.M. Millam, S.S. Iyengar, J. Tomasi, V. Barone, B. Menonucci, M. Cossi, G. Scalmani, N. Rega, G.A. Petersson, H. Nakatsuji, M. Hada, M. Ehara, K. Toyota, R. Fukuda, J. Hasegawa, M. Ishida, T. Nakajima, Y. Honda, O. Kitao, H. Nakai, M. Klene, X. Li, J.E. Knox, H.P. Hratchian, J.B. Cross, C. Adamo, J. Jaramillo, R. Gomperts, R.E. Stratmann, O. Yazyev, A.J. Austin, R. Cammi, C. Pomelli, J.W. Ochterski, P.Y. Ayala, K. Morokuma, G.A. Voth, P. Salvador, J.J. Dannenberg, V.G. Zakrzewski, S. Dapprich, A.D. Daniels, M.C. Strain, O. Farkas, D.K. Malick, A.D. Rabuck, K. Raghavachari, J.B. Foresman, J.V. Ortiz, Q. Cui, A.G. Baboul, S. Clifford, J. Cioslowski, B.B. Stefanov, G. Liu, A. Liashenko, P. Piskorz, I. Komaromi, R.L. Martin, D.J. Fox, T. Keith, M.A. Al-Laham, C.Y. Peng, A. Nanayakkara, M. Challacombe, P.M.W. Gill, B. Johnson, W. Chen, M.W. Wong, C. Gonzalez, J.A. Pople, Gaussian 03, Revision B.04, Gaussian Inc., Pittsburgh, PA (2003)
- 19 A.V. Rode, E.G. Gamaly, A.G. Christy, J.G. Fitz Gerald, S.T. Hyde, R.G. Elliman, B. Luther-Davies, A.I. Veinger, J. Androulakis, J. Giapintzakis, *Phys. Rev. B* **70**, 054407 (2004)
- 20 F. Banhart, *Formation and Transformation of Carbon Nanoparticles under Electron Irradiation* (The Royal Society, London, 2004)
- 21 G.D. Lee, C.Z. Wang, J. Yu, E. Yoon, K.M. Ho, *Phys. Rev. Lett.* **91**, 265701 (2003)